EVALUATION OF REPLICATION METHODS FOR THE STUDY OF HAZ STRUCTURES IN MULTIPASS WELDMENTS AND THE PREPARATION OF EELS STANDARDS

FINAL REPORT

by

D. Paine and G.C. Weatherly

Department of Metallurgy and Materials Science
University of Toronto
Toronto, Ontario
M5S 1A4

Work on this project was conducted under the auspices of PMRL, CANMET, EMR, Canada

DSS File Number: 26SQ.23440-3-9025

DSS Contract Serial Number: 1SQ83-00020

CANMET SCIENTIFIC AUTHORITY: Dr. M.J. Godden

October 1984

EXECUTIVE SUMMARY

A carbon extraction replica technique was developed for studying the distribution of carbo-nitride particles in HSLA steel weldments, both from single-pass and two-pass regions in the heat affected zone. The method was applied successfully to a Ti-Nb bearing steel and it was demonstrated that a single replica can sample the weld metal, fusion line boundary and the HAZ to a distance greater than 1 mm from the boundary. The variation of particle composition with particle size was measured for both the single and two-pass regions: the average particle size and Ti content in the particles increased as the fusion line was approached. At a distance of ~0.8 mm from the fusion boundary in the single pass region and ~0.3 mm in the two pass region the average particle composition was similar to that found in the parent plate material.

A technique was developed for the preparation of silicon monoxide replicas from HSLA steels to measure the C:N ratio in carbo-nitride particles. A number of thin film standards were prepared for light element analysis using electron energy loss spectroscopy. Spectra were obtained from these standards using the PMRL CANMET analytical electron microscope facility.

RESUME :

Une technique reproductible dans l'extraction du carbone a été développée pour l'étude de la distribution des cristallites nitrure et carbure à la soudure d'un acier HSLA. L'analyse des deux composés est obtenue directement après un passage ou après deux passages sur la région affectée par la chaleur. La méthode a été appliquée avec succès sur un roulement à bille en acier dopé au titane-nobium Ti-Nb, il a été démontré que la reproductibilité peut être atteinte aussi bien avec le métal de la soudure que celui de la ligne de fusion ou des parties exposées à la chaleur, jusqu'à une distance supérieure à I mm de cette ligne de fusion. La variation de la composition des cristallites selon leurs tailles et leurs concentrations en titane a été mesurée aprés un ou deux passages sur la région concernée. La taille moyenne des cristallites et leur teneur en titane augmentent de plus en plus jusqu'à la ligne de fusion. A une distance de 0,8 mm de cette ligne et de 0,3 mm pour le second passage, la composition moyenne des cristallites était similaire à celle obtenue dans l'acier initial.

Une technique a été développée pour la préparation d'acier HSLA au monoxyde de silicium pour en mesurer le rapport carbone sur azote C/N de cristallites au carbo-nitrure. Plusieurs films étalons de faible épaisseur ont été préparés pour une analyse élémentaire par spectrographie d'arc. A partir de ces étalons, des spectres ont été réalisés au microscope électronique analytique disponible- le PMRL CANMET-

I. GENERAL INTRODUCTION

Under the terms of the work statement in Appendix G of this subcontract, work was to be performed in two areas: (a) development of techniques for the study of the coarse grain HAZ and a peak temperature region corresponding to ~1000°C in multipass weldments, and (b) development of standards for EDX, EELS and light element analysis (C, N) in particles.

In the first part of the contract approximately 4 multipass welds, prepared in 350 WT steel at 50 mm thickness, were to be provided by STELCO and PMRL. These welds were to be made in the specific weld configuration noted in the Welding Institute project "Normalized Steels with Improved HAZ Toughness". A copy of this document was provided to the authors, together with 2 multipass weldments which had been fabricated at Stelco. Unfortunately the weld profile in the samples (both parallel and transverse to the welding direction) precluded taking samples from planar sections cut parallel to the nearly vertical flat fusion line of the weldment. After consultation with Dr. M.J. Godden at PMRL, it was decided to proceed with an alternative method of examination, whereby samples were removed from transverse sections including the weld metal, fusion line and HAZ. This method, and the results obtained, are described in Section II of this report.

In the second part of the contract, a technique for the preparation of SiO replicas was developed and tested on a Ti-bearing steel known to contain (Ti(C,N) particles. This is described in Section III. Finally a number of EELS and EDX standards suitable for the characterization of typical carbo-nitride particles in HSLA steels were prepared. At the

time of writing of this report, the examination of these standards has been completed, but the analysis of the raw data (being done by Dr. T. Malis, CANMET) is as yet unfinished. The range of standards and the method of their fabrication are described in Section III.

II. WELD HAZ PRECIPITATE CHARACTERIZATION

II-1. Introduction

In this section of the report the technique developed for obtaining carbon replicas of the heat affected zone (HAZ) of multipass weldments is described. The task outlined in the D.S.S. specification required obtaining replicas from at least two regions of the HAZ, including the coarse grain HAZ immediately adjacent to the weld fusion line and a suitable region subject to a peak temperature of the order of 1000°C. A detailed description of a technique for doing this follows. Results are presented which clearly show how the distribution of HAZ precipitate size and composition changes as a function of distance from the fusion line of the weld. Two regions of the HAZ were studied. The first region, which will be called the one pass region, involves those HAZ regions which have experienced the thermal pulse of a single weld bead. The second region, called the two pass region, are those regions where the effects of the thermal cycle of two weld beads overlap.

II-2. Experimental Details

II-2.1. Materials

One multipass arc weld was used to develop the technique. The weld, provided by STELCO and PMRL, was to have been made in the specific weld configuration noted in the Welding Institute project "Normalized Steels with Improved HAZ Toughness". The welded plate, 50 mm thick, was provided by STELCO and was concast with a normal weight % composition of: 0.07 C, 1.43 Mn, 0.003 P, 0.004 S, 0.29 Si, 0.25 Ni, 0.25 Cr, 0.075 V, 0.02 Nb, 0.011 Ti, and 0.007 N. The multipass arc weld had an energy input of 2 kJ/mm per pass.

II-2.2. Sample Sectioning

Figure 1 shows in section one half of the thickness of the weld provided. This figure demonstrates that the technique used by STELCO to weld the plate could not provide the planar HAZ/fusion line interface described in the Welding Institute project previously mentioned. In order to characterize this non-planar interface, extraction replicas from the cross-section shown in Figure 1 were used. The decision to take replicas from the profile of the weld rather than from a plane parallel to the line of the weld, allowed the development of a technique which should be equally effective for welds with the specified planar fusion boundary.

II-2.3. Preparation of the Weld Sample

A section of the weld, approximately 2 cm long was cut from the plate. The unaffected plate material was also trimmed off to make the weld more manageable for metallographic preparation. Figure 1 shows the resulting sample.

The sample was prepared by standard metallographic techniques, i.e. grinding with 120, 240, 400, and 600 grit SiC paper followed by polishing with 1 μm Al_2O_3. The polished sample was then etched using 5% nital for approximately 7 seconds. The etch exposed the weld and made the HAZ visible.

The sample was carbon coated using a standard C evaporation technique. A pressure of 6 mPa and a current high enough to cause an arc to be struck was used. The current was applied four times for two seconds each time. The sample was placed 7-9 cm from the graphite rod. These conditions were somewhat variable, but the objective in each case was to use as little C as possible, while maintaining the integrity of the coating.

II-2.4. Definition of Region of Interest

II-2.4.2. Coarse Grain HAZ

The fusion line could be seen through the carbon layer. Three or four regions of interest were chosen that involved one or two pass areas in the HAZ immediately adjacent to the fusion line. Since a TEM Cu grid is 3 mm in diameter, and the area visible in the TEM is 2 mm or less in diameter, a sharp point was used to scribe lines through the C layer into the underlying metal, so that the area to be sampled was well defined.

For one pass regions, a rectangle with two 1 - 1.5 mm sides parallel to the fusion line was scribed. The fusion line was chosen to fall close to one of the sides but was included in the area between the two sides, which were made 2 - 2.5 mm apart. When the final two sides (i.e. the sides approximately normal to the fusion line) were scribed, a slight taper away from the fusion line made finding the end closest to the fusion line easier (see Fig. 16 at the end of the report).

To sample the two pass region, it proved necessary to orient the replica such that the apex of the two pass "V" where the weld beads overlapped could be located. Furthermore, it was important to be able to determine, on the replica, while viewing in the electron microscope, the direction which would allow the observer to pass directly away from the fusion line. This is the direction in which the HAZ will be affected equally by both weld beads. To allow the accurate orientation of the replica, two techniques proved useful.

The first technique required less effort and could be done relatively quickly but may not give a high degree of confidence that the apex of the "V" and the direction determined are accurate. In a manner similar to

that described for the one pass weldments, lines were scribed onto the carbon film which enclosed part of the fused weld metal. In this case, however, a trapezoid was formed which had the apex of the two pass weld "V" close to the centre of the shortest of its two parallel sides. The opposite parallel side was positioned so that its centre was also approximately lined up with the apex of the weld (see Fig. 16). This technique is further described in Section II-2.6.1.

The alternative and more accurate method involved making microhardness indentations which started at the apex of the two pass weld and followed a linear path away from it, directly towards the unaffected plate metal (Fig. 16). A standard microhardness indenter with a diamond head and a 10 kg load was used sucessfully, with a separation of 70-100 μm between impressions. When this technique was used, the orientation of the replica was found by searching the replica for the microhardness indentations. The technique used to do this is described in Section II-2.6.1.

II-2.4.2. Fine Grained HAZ

Results shown later in this report indicate that there is little effect on the Ti/Nb precipitate distribution further than 1 mm from the fusion line in the 2 kJ/mm weld case. It is, however, possible to characterize precipitates in the region of the HAZ which are not close enough to the fusion line to be included in the first replica if this proves necessary. This was done by scribing a second replica trapezoid adjacent to the first, onto the surface of the steel. As before, the trapezoid was scribed such that the non-parallel side tapered towards the fusion line. In this instance, two replicas were removed, as described earlier, the first which included the fusion line and the second which

included the region further away. The centre of the shortest parallel side of the carbon replica was determined at very low magnification in the TEM or by optical microscopy, while the direction to the opposite side was determined with respect to the bars of the copper grid.

II-2.5. Carbon Extraction Procedure

The extraction procedure itself first involved painting the C-coated surface with lacquer leaving the scribed areas of interest exposed. A red Microstop acetone-soluble lacquer was used but a clear lacquer may improve the visibility of the C films once they are lifted off.

For large samples, it was found that forming a "dish" using electricians' tape, in which the sample surface was the bottom, worked well. The tape was first folded one third back on itself in the longitudinal direction then applied around the weld sample to form the dish. Lacquer was used to seal the tape/metal corners in the "dish" to prevent the electrolyte from leaking out.

The "dish" formed by electricians' tape and the surface of the sample was filled with electrolyte using an eye dropper. The electrolyte consisted of 10% perchloric, 70% ethanol, 10% butylcellusolve, and 10% water. A standard electropolishing set up was used to detach the replica from the steel surface.

The anode of the electropolishing set-up was secured to the steel weld while the cathode was attached to a length of 0.75 mm diameter stainless steel wire. This wire was held just submerged in the electrolyte, parallel to the steel surface, with the current off. Slowly, the current was increased until bubbles began to form at the cathode. (This current

will depend upon the area of the electrodes used.) After about 5 minutes, the carbon film appeared to darken. By moving the cathode over a particular area, particular carbon trapezoids could be encouraged to curl and detach from the steel surface. At this point, the curled C film was removed from the electrolyte using a coarse TEM Cu grid. Unless all the areas of interest are of the same type (one pass or two pass) and the particular position in the weld (near the top, bottom, or centre) does not matter, the C film must be carefully followed to see which weld region it comes from. A large magnifying lens with a lamp proved helpful for this step. The carbon films were stored in watchglasses containing ethanol until all of them had been collected; each was placed in its own designated watchglass. To open the curled C films, the replicas were gently placed into a 50-50 mixture of ethanol and distilled water. The carbon film floated on the surface of the water/ethanol mixture and was scooped out using 200 or 400 mesh Cu TEM grids. [N.B. If the microhardness indentation technique is used, 200 mesh grids will make the microhardness indentation impressions easier to find in the electron microscope.]

II-2.6. Electron Microscopy

II-2.6.1. Preliminary Observation and Orientation

Preliminary observations of the extraction replicas were made using a Philips EM300 TEM. During these observations, the replica was characterized with respect to orientation. First, the weld metal region was found. This region was easily identified because of the large spherical inclusions associated with the weld pool. The interface between the fusion metal and the HAZ was clearly defined by a zone depleted of

inclusions or precipitates. This region, also described in Section II-3.1, was usually less than 30 μm wide and appeared on the replica as a featureless region. Once the depleted zone was identified for the one pass region, it was relatively easy to move normal to this interface during analysis of the HAZ.

For two pass regions, the centre of the two pass "V" had to be located. The first two pass technique described in Section II-2.4.1 ensured that the apex of the two pass "V" would be located along the shortest parallel side of the C film trapezoid. The centre of this side could be found by counting the number of grid squares it covered. Using an optical microscope, it was possible to quickly determine the centres of the two parallel sides. A line connecting these centres is the desired analysis path. This line should also be normal to the edge of the shortest side of the carbon trapezoid. The angle this line made with the grid bars was also noted to allow the direction to be maintained in the electron microscope.

The alternative method, described in Section II-2.4.1, involved the use of microhardness indentations. In the TEM, the line of microhardness impressions could be found through careful searching with the specimen steeply inclined (>30°) with respect to the electron beam. Unfortunately, even if 200 mesh grids were used, a large fraction of the indentations were hidden by the grid bars. Furthermore, the indentation impressions were very difficult to identify using the STEM mode on the HB5.

II-2.6.2 X-ray Microanalysis

Energy dispersive X-ray microanalysis of the particles in the HAZ was carried out in a HB5 dedicated STEM. The first grid square closest to the depleted zone was analyzed with subsequent grids being analyzed at regular intervals away from the fusion line. The correct direction relative to the grid bars was determined as described in the previous section. Within each of the grid squares studied, 20 particles chosen at random were analyzed. The size of each particle was determined directly by measurement on the STEM CRT screen. The grid squares allowed a well defined region to be used while 20 individual particle analyses give a good idea of the local size-composition distribution. For higher statistical significance, many more particles in each square could be analyzed. The x-ray spectrum obtained for each particle was stored and later analyzed. Analysis of the spectrum used the standard Cliff-Lorimer ratio of intensities corrected by a K factor. The two main elements of interest were Nb and Ti, which have a K_{TiNb} factor of 0.51 for the HB5 as determined from standards used in this work (see later). The results were plotted as the weight ratio of Nb/Nb+Ti against average particle diameter.

II-3.0 Results

II-3.1 Depletion Zone

The series of TEM photomicrographs shown in Figures 2, 3, and 4 demonstrate that the fusion line region in the C replica can be readily determined in the electron microscope at relatively low magnifications. In Figures 2 and 3 large spherical particles typical of weld pool inclusions can be seen. EDX analysis confirmed that these were weld pool inclusions since their composition included elements such as Al, Si, Ti,

and Mn. The columnar grain shape typical of the weld pool can also be seen in the structure of the C film. Immediately adjacent to the weld pool region in the figures, was an area on the C replica which was relatively featureless with no precipitates of any type visible. This region which will be called the depleted or featureless region, was approximately 30 μm wide. Beyond the depleted zone, a region containing Fe_3C and Ti,Nb(C,N) cuboids could be seen. This area of the HAZ is of interest in this report. The significance of the depleted zone, whose origin is obscure, is that it allows a clearly defined starting point for analysis of HAZ precipitates.

II-3.2 HAZ-TEM Observations

The photomicrographs shown in Figures 5, 6 and 7 are representative examples of a series of photomicrographs which indicate the changing size distribution of precipitates as one moves away from the fusion line on the C replica. The trend is clear; a larger number of coarser cuboid precipitates were present near the fusion line. As the distance from the fusion line increases, and consequently, the maximum peak temperature decreases, the number of large cuboidal particles decreases. Throughout the HAZ there was a dispersion of fine precipitates (20-100 nm in diameter) whose apparent density decreased near the fusion line. It is likely that the majority of these particles are present because there has been insufficient time during the heating cycle to allow them to dissolve.

II-3.3 Size-Composition Distribution

II-3.3.1 Plate Material

The size-composition analysis of Ti,Nb(C,N) particles in the unaffected plate material is presented in Figure 8 where the ratio Nb:Nb+Ti

is plotted against the average particle diameter. This figure shows that the plate material has, for the most part, Nb-rich particles in the 15-40 nm size range. There were occasional coarser Ti-rich particles also visible.

II-3.3.4 One Pass Zone

The one pass zone described earlier was analyzed using STEM-EDX. Regions near the fusion line, 252 μm, 567 μm, 882 μm, and 1197 μm from the fusion line were analyzed. The results are presented in Figure 9, which also compares the trends shown with the base plate analysis. Near the fusion line, the Ti content has increased considerably compared to the parent plate. In addition, a much greater scatter of particle diameters with a large number of coarse particles can be seen. As the distance from the fusion line increases the Nb content increases and both the composition and size distribution begins to resemble that of the parent plate at ∿800 μm from the fusion line. To ensure that this trend was representative, a second analysis of a different one pass region was carried out. This gave the results summarized in Figure 10. These results were very similar and confirmed the trend already described.

II-3.3.3 Two Pass Region

The analysis of the two pass zone gave the particle size-composition distribution shown in Figure 11. Again, as in the one pass analysis, a distribution of coarser Ti-rich particles was observed near the fusion line. The Ti content and average size of the particles dropped as the distance from the fusion line increased. The particle size-composition distribution was similar to that of the parent plate at a shorter distance (∿300 μm) from the fusion line than it did in the one pass situation.

II-3.4 Temperature Range Sampled

The exact temperature profile on HAZ adjacent to the fusion line can be determined fairly accurately for single pass, 2- or 3- dimensional heat transfer cases. For the situation in this study, however, this determination is much more difficult because the weld involves several passes located at different positions in the weld groove, all of which complicate the analysis. Roughly, however, it is known that the HAZ adjacent to the fusion line etches uniformly up to the region which has experienced a peak temperature of 730°C. This etched region extends ∿2 mm from the fusion line in the 2 kJ/mm samples used in this study. In most cases, as we have demonstrated, it is possible to study an area which extends 1000-1100 μm, i.e. approximately 1 mm or more from the fusion line. Assuming that the peak temperature (T_p) reached at any point y in the HAZ varies with the temperature according to the familiar law $\frac{1}{T_p - T_o} - \frac{1}{T_M - T_o} = Ay$, where T_o is the preheat, T_M is the melting temperature and A is a constant,* a temperature of 1000°C should be reached ∿1 mm from the fusion line in this case. At this distance, the particle composition-size distribution is very similar to that of the unaffected parent plate. This conclusion is of course limited to the particular heat input/parent plate combination studied here, and does not consider possible variations in the C:N ratio in the particles.

II-4 Summary

A spatially accurate and statistically meaningful technique for the analysis of HAZ particles in multipass weldments has been developed. Composition versus particle size distributions were determined as a function of increasing distance from the fusion line for both single and

* A can be determined approximately from the position of the 730°C isotherm.

two pass regions of the HAZ. Distances up to ~1 mm from the fusion line can be routinely analyzed. A modification of this technique to allow analysis of regions at a distance greater than 1 mm from the fusion line was suggested. The technique can be used to readily analyze two regions - the one pass region which involves essentially the effects of a single weld bead and the two pass region which includes the overlapping effects of two weld beads.

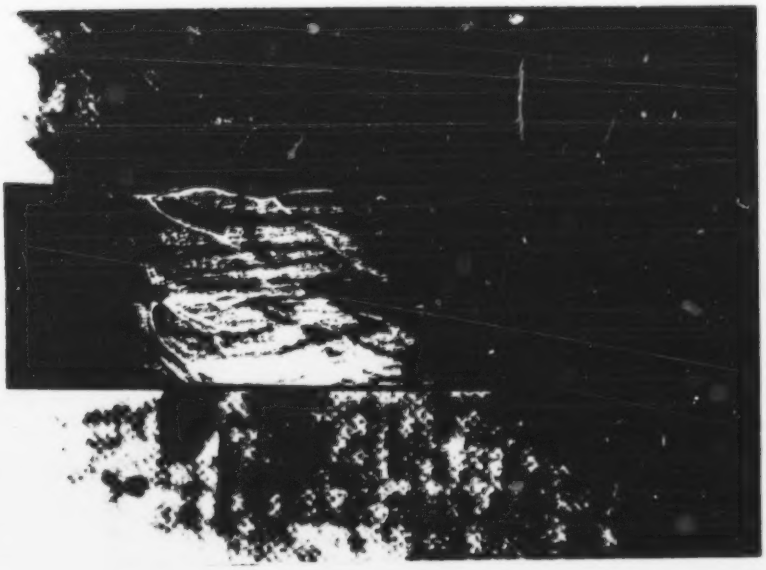

Fig. 1. Optical micrograph showing the transverse section of the weld. Note the lack of planarity at the vertical fusion line on the left hand side (x 1½).

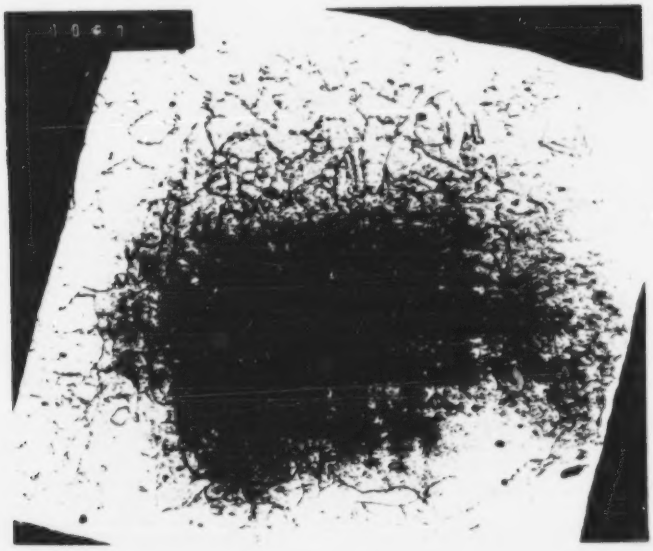

Fig. 2. This figure and the next two figures show the typical appearance of a carbon extraction replica at the weld metal-fusion-line-HAZ junction. In this figure, large spherical inclusions typical of a weld metal are visible (x 2650).

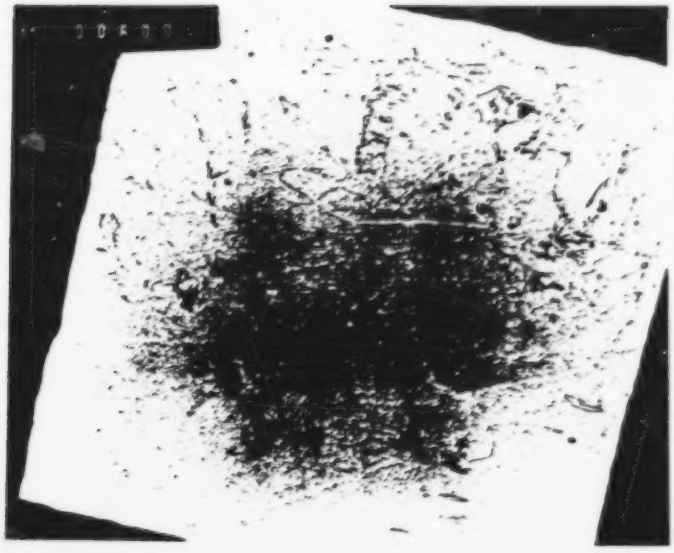

Fig. 3. Area adjacent to Fig. 2 showing the weld metal and the "featureless" zone (x 2650).

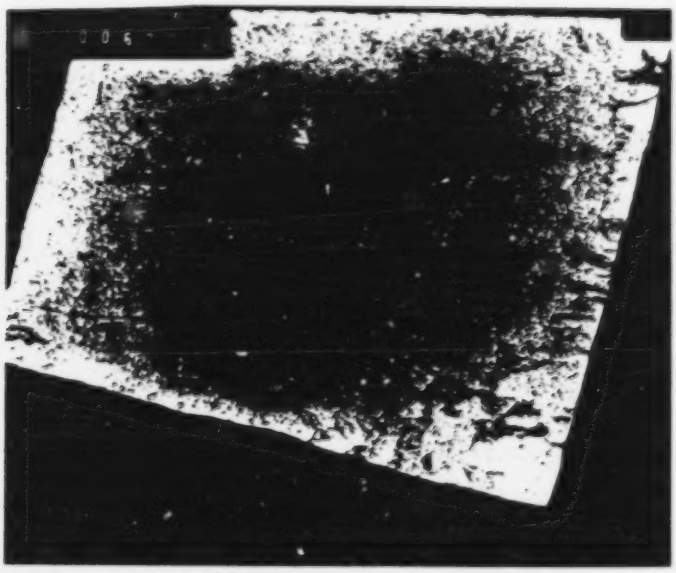

Fig. 4. Area adjacent to Fig. 3 showing the "featureless" zone and the start of the HAZ with discernible precipitation effects (x 2650).

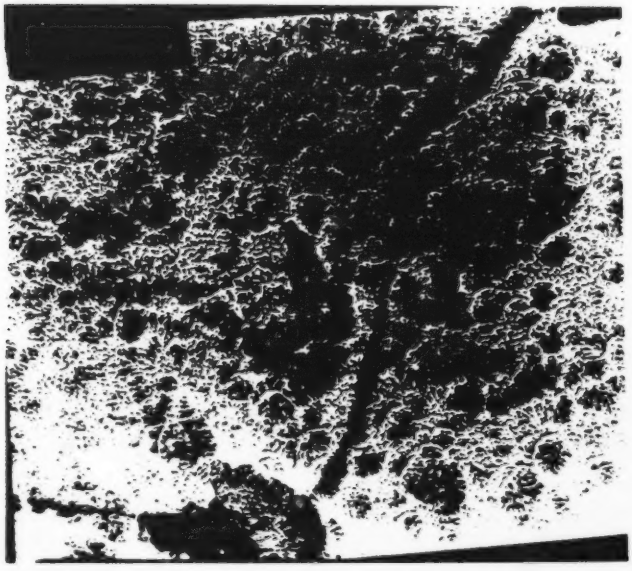

Fig. 5. Distribution of particles in the HAZ region, ∿830 μm from fusion line, single-pass region (x 80,500).

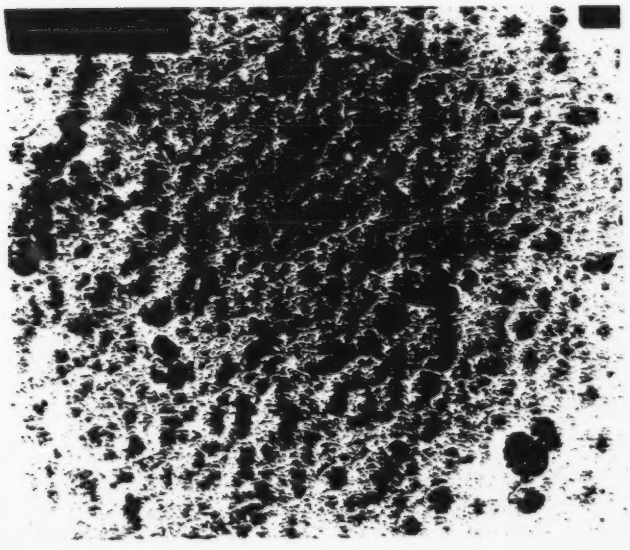

Fig. 6. As Fig. 5, ∿450 μm from fusion line (x 55,000).

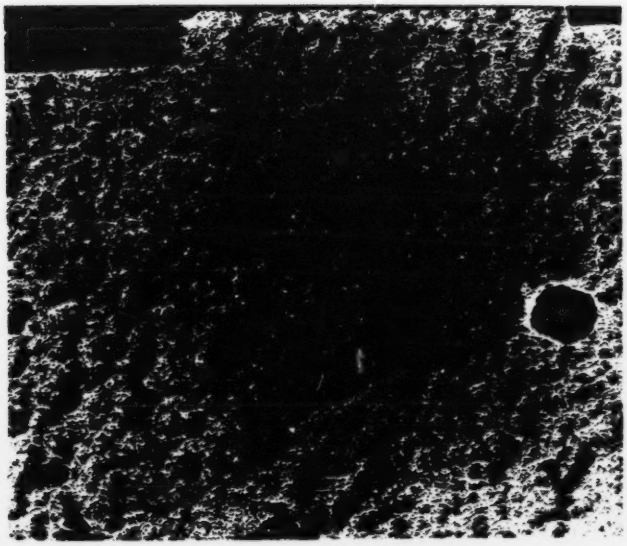

Fig. 7. As Fig. 5, ∿128 μm from fusion line (x 55,000).

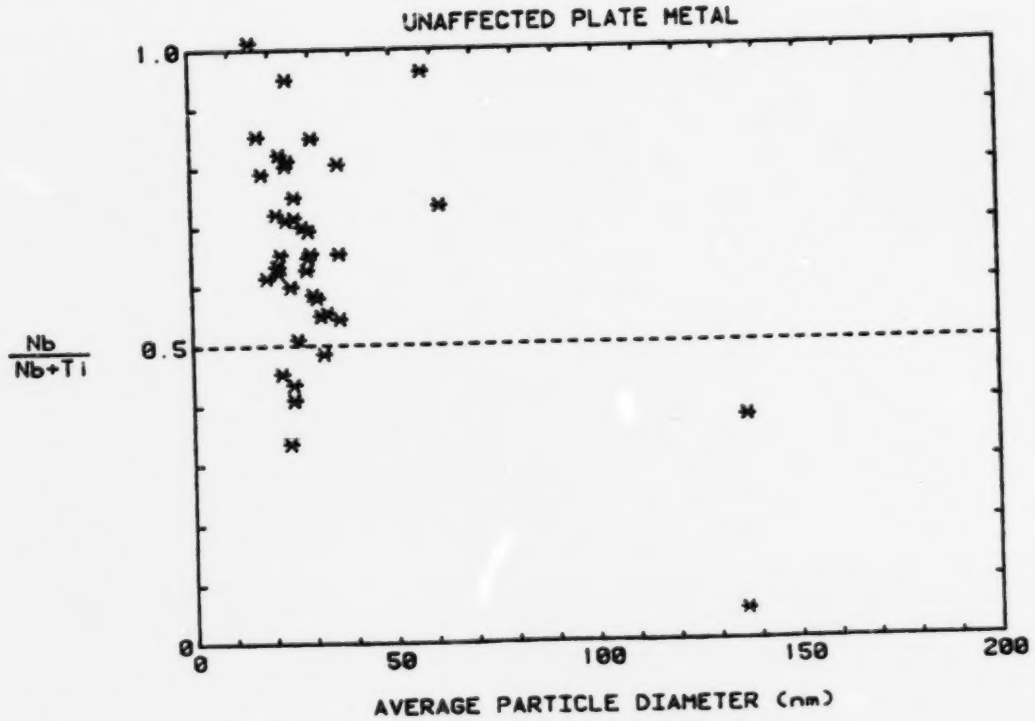

Fig. 8. Particle size-particle composition relationship in the parent plate. Apart from a few coarser Ti-rich particles, the majority of the particles are Nb-rich.

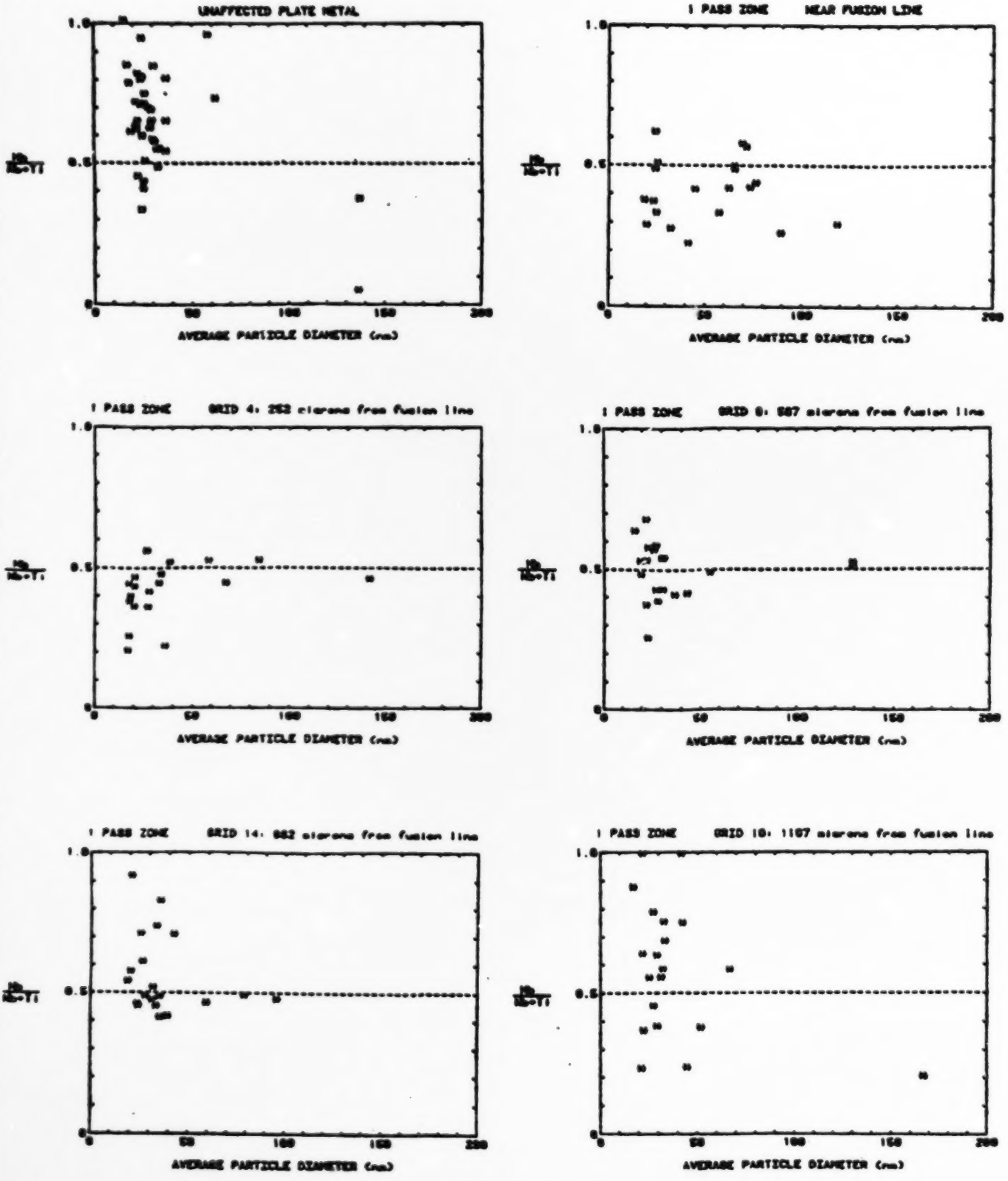
UNAFFECTED PLATE METAL
1 PASS ZONE NEAR FUSION LINE
1 PASS ZONE GRID 4: 252 microns from fusion line
1 PASS ZONE GRID 8: 567 microns from fusion line
1 PASS ZONE GRID 14: 862 microns from fusion line
1 PASS ZONE GRID 18: 1167 microns from fusion line
AVERAGE PARTICLE DIAMETER (nm)

Fig. 9. Comparison of particle composition-size relationship with increasing distance from the fusion line. Note changes close to fusion line.

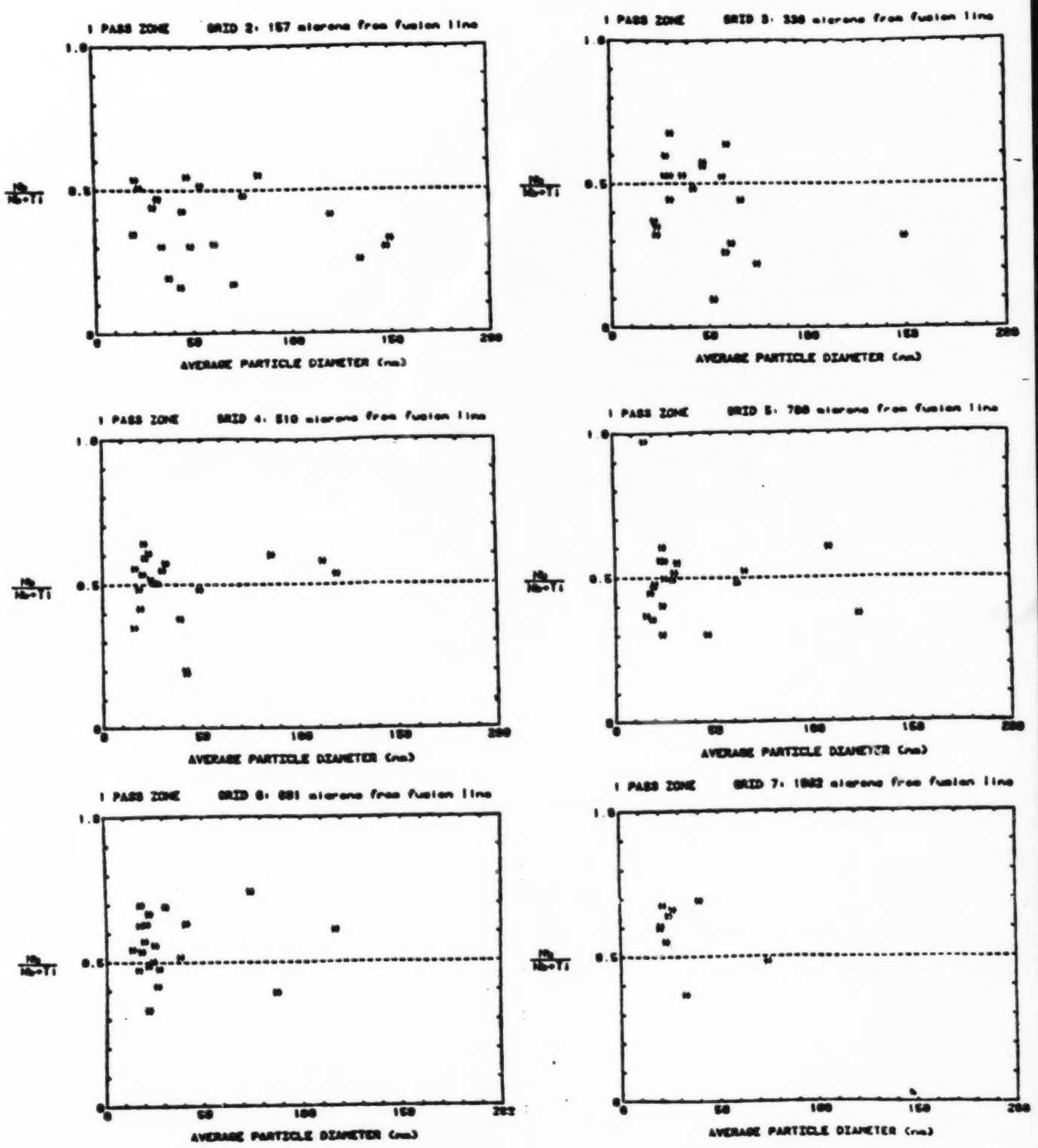
1 PASS ZONE
GRID 2: 157 microns from fusion line
1 PASS ZONE
GRID 3: 330 microns from fusion line
1 PASS ZONE
GRID 4: 510 microns from fusion line
1 PASS ZONE
GRID 5: 700 microns from fusion line
1 PASS ZONE
GRID 6: 891 microns from fusion line
1 PASS ZONE
GRID 7: 1082 microns from fusion line
AVERAGE PARTICLE DIAMETER (nm)

Fig. 10. As Fig. 9, for another single pass region in the HAZ.

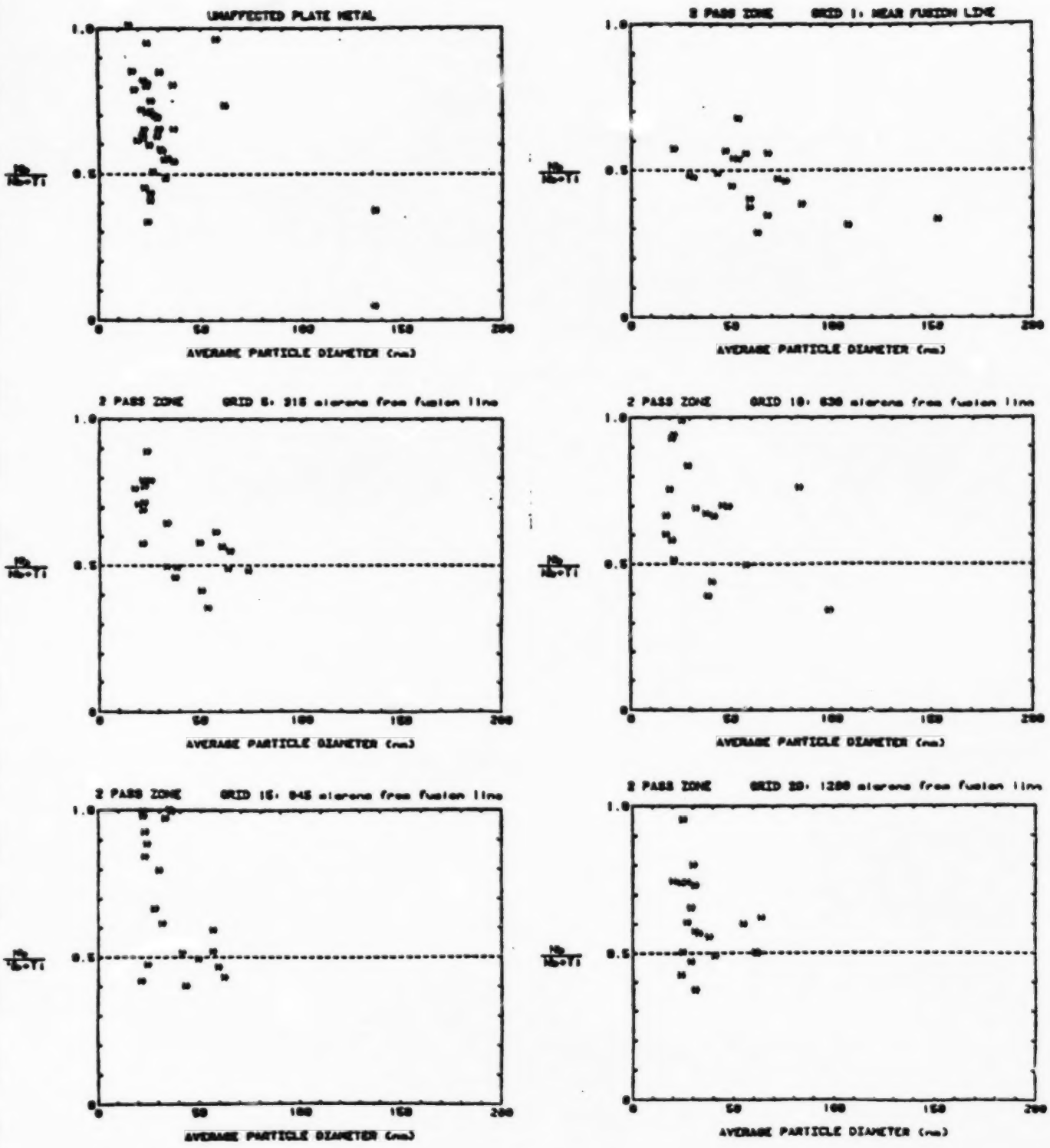
UNAFFECTED PLATE METAL
2 PASS ZONE GRID 1: NEAR FUSION LINE
2 PASS ZONE GRID 8: 315 microns from fusion line
2 PASS ZONE GRID 10: 630 microns from fusion line
2 PASS ZONE GRID 15: 945 microns from fusion line
2 PASS ZONE GRID 20: 1260 microns from fusion line
AVERAGE PARTICLE DIAMETER (nm)

Fig. 11. As Fig. 9, for two pass region of the HAZ.

III. REPLICATION TECHNIQUES AND EELS STANDARDS

III-1 Introduction

The purpose of this section of the work was twofold; firstly a method for the preparation of replicas was to be developed which could be used for EELS analysis of light elements, particularly the C/N ratio of HAZ particles. The technique studied concentrated on SiO as the replication medium. The second purpose of this section was to develop EELS standards which would allow the quantification of experimental data obtained by EELS, especially with respect to HSLA steels. The single most important parameter when considering quantitative EELS is the specimen thickness. Both standards and replicas must be less than 500 nm thick to provide useful EELS data.

III-2. Silicon Monoxide

III-2.1 Introduction

The replication work concentrated on the use of Si-based replica films. Silicon monoxide, a once-common replication material, was considered. Single stage replicas were produced under several conditions. Since SiO films on steel are invisible, methods of making them more readily visible for replication were developed. The stability of SiO films in the electron microscope was also a problem and this was addressed.

III-2.2 Experimental Details

III-2.2.1 Materials

All replication techniques were tested on a standard Ti-bearing HSLA steel which had undergone a Gleeble heat treatment designed to

simulate a peak temperature of around 1350°C. The steel was provided as a mounted sample which included the area that had experienced the peak temperature. The SiO was purchased from a chemical supply house as coarse 2 cm-sized chunks.

III-2.2.2 Sample Preparation and SiO Evaporation

The steel was prepared metallographically using the standard procedure described in Part II of this report. The coarse silicon monoxide particles were crushed to provide sub-millimetre-sized particles. These particles were then placed in a tungsten wire basket in a standard vacuum evaporator. The optimum results were achieved with the best available pressure of around 6 mPa. Under vacuum, the tungsten basket was resistively heated by slowly increasing the current through the basket. As the current was increased, the vacuum degraded, indicating that the silicon monoxide was evaporating. A current of 5-10 Amps was passed for 2-3 mins to complete the evaporation process. The thickness of the SiO was varied by filling the tungsten basket as full as possible each time and increasing the distance of the sample from the source. Ultimately, a distance of 5-7 cm was found to give the best results.

III-2.2.3 Gold Sputtering

In order to make the film on the surface of the steel visible, gold was sputtered onto the surface of the SiO coated steel sample. This approach has the added benefit of stabilizing the SiO films after they have been removed. An Ar ion beam sputterer with a Au target was used to deposit the Au. The thickness of the deposited film could be determined by specifications provided with the sputter unit. These thicknesses varied between 10-120 nm. When the films were removed using the technique

described in the next section, it was seen that a continuous film of Au could not be produced even with Au thicknesses as great as approximately 90 nm (see Figure 12). Since a maximum thickness of 50 nm is desirable, the Au approach is of limited value. Although the Au islands stabilize the film they also increase its net thickness. Gold does, however, make the SiO_x films visible while on the steel.

III-2.2.4 Single Stage SiO_x Extraction

Ultimately, a successful procedure for producing single stage SiO_x replicas was developed. The reliability of the technique, however, was low and further work should be done to develop a better understanding of the parameters involved. The procedure was identical to that described in Part II, Section II-2.5 except a grid work was scribed into the surface of the sample and only the electricians' tape was sealed with Microstop lacquer.

The SiO was first evaporated onto the sample as described in the previous section. The only difference in procedure when dealing with SiO_x films rather than C films involved using a slightly lower current. Once again, incipient bubble formation on the cathode was used as the critical current criteria. Much longer electropolishing times were required when lifting SiO_x films, usually in excess of twenty minutes.

As the film was being lifted from the steel surface, very little was visible; for the most part the SiO_x film remained transparent and invisible until the end. Eventually the surface appeared darker and deeply etched by the electrochemical attack. This usually signified that the electrolyte had penetrated under the entire SiO_x film and could be removed. Removal of the films was done by flushing the steel sample's

surface with alcohol over a large watchglass. When the watchglass was placed over a black background, the SiO_x films could be seen if viewed obliquely. The films were not usually rolled up as was observed with the C films and they proved to be much more fragile. For this reason the films were washed in a solution containing 75% ethanol, 25% water and were collected on 400 mesh grids.

III-3. Results

While some films disintegrated under the electron beam during observation, others managed to survive for several weeks. Figures 12, 14 and 15 show a moderately stable film in which cracking can be seen. Very thick SiO_x films, i.e. those placed nearest to the evaporator source, proved to be useless as it was impossible to detect the presence of precipitates in the structure of the film. Moderately thick films appeared to suffer more cracking than thinner ones prepared at a greater distance from the SiO source. This may mean that stresses developing as the thickness of the film increases are causing the film instability. Analysis of the film thickness (by EELS methods) of the most stable SiO replica produced to date indicated a thickness of 35 nm. This has not been uniquely established, however; trials involving an oscillating crystal thickness monitor would resolve this point.

The question of optimum film composition was also considered. The most stable and structureless SiO film produced to date was analyzed using EELS. The EELS results, however, were inconclusive; using the K edge for Si, the Si:O ratio was 1 to 1 indicating SiO. Using the less reliable L edges indicated a composition of SiO_2. More work on this aspect of the problem is also recommended. Using this same film, the presence of C and N in extracted carbo-nitride particles from the HSLA steel was clearly established (see next section).

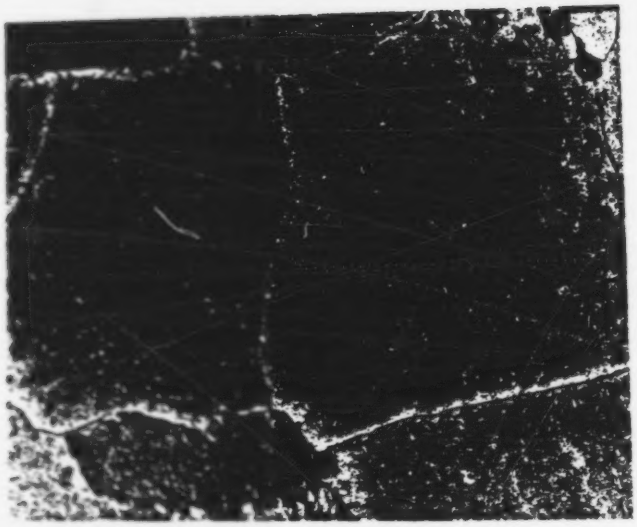

Fig. 12. Au shadowed SiO extraction replica showing the discontinuous nature of the Au film (x 8000)

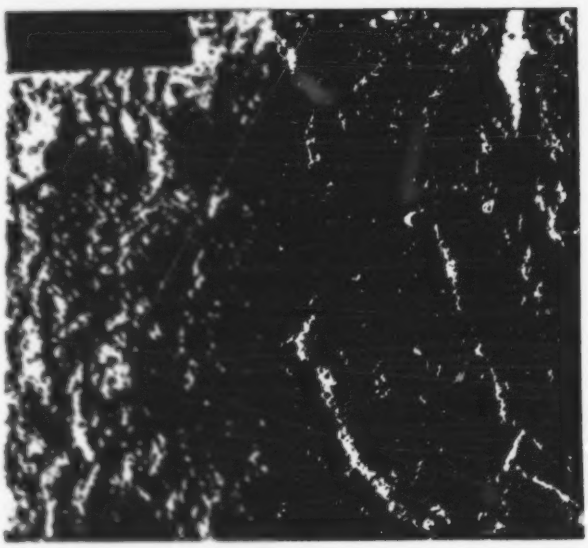

Fig. 13. SiO extraction replica of Ti-bearing steel showing extracted carbo-nitride particles (x 8000).

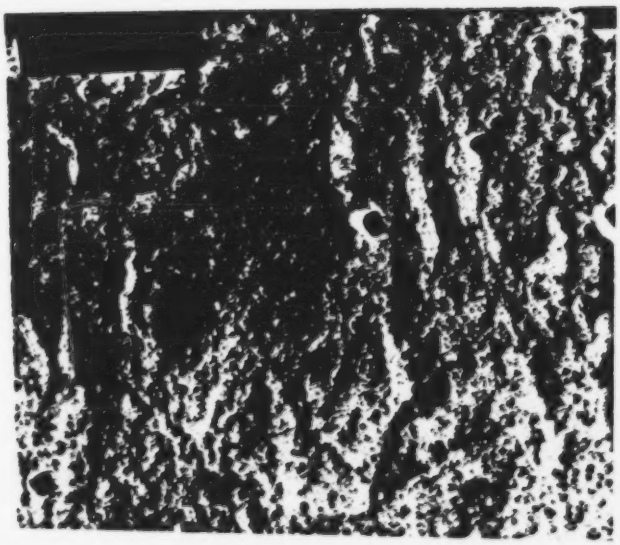

Fig. 14. As Fig. 13 (x 10,000).

Fig. 15. As Fig. 13, note the tendency of the replica to crack adjacent to the extracted particles (x 30,000).

III-4. EELS Standards

Standards were prepared by a number of techniques, with the co-operation of a number of different investigators (Drs. J. Titchmarsh, M. Ball and T. Malis). Spectra from thin areas of the samples were recorded using a Gatan spectrometer fitted to a Philips EM400T at PMRL, CANMET. In the list that follows, the sample preparation techniques are recorded and the particular conditions used for each sample are noted in Table I. The Ti-Nb thin film standard was prepared by a sandwich technique as described below.

Ti/Nb standards were produced by fabricating sandwiches consisting of a layer of Ti onto which a layer of Nb was deposited. Three film thicknesses were produced in a ratio by weight of Ti/Nb of 0.277. The thicknesses were 30 nm, 100 nm and a set of films whose thickness was greater than 100 nm.

The procedure used a multisource evaporator. $BaCl_2$ was first evaporated from a resistively heated boat onto a standard glass slide. Ti was evaporated onto the $BaCl_2$, also using resistance heating. The thickness of the layer was continuously monitored using a crystal oscillator. If the source was kept at an appropriate distance, the film thickness could be followed with an accuracy of about 0.1 nm. After the required thickness of Ti had been deposited, Nb was evaporated by using an electron gun. The thickness of this layer was also monitored.

In order to strip the film, one end of the glass slide with the $BaCl_2$/Ti/Nb sandwich was placed into a dish of water. With the glass slide inclined at an angle of 30° to the water surface, the water slowly dissolved the $BaCl_2$, thus detaching the films which floated in the dish. The film sandwiches of Ti/Nb were then scooped out of the dish onto Cu grids.

TABLE I

Record of EELS Samples

Spectrum Number	Sample	Sample Thickness ($\frac{t}{\lambda}$)	Convergence Angle (α)	Collection Angle (β)	Notes
FNBUM1	$Fe_{40}Ni_{40}B_{20}$ ultramicrotomed	0.36	2 mrad	5.8 mrad	Area analyzed $\sim 0.04\ \mu m^2$
FNBUM2	"	"	"	"	Area analyzed $\sim 1\ \mu m^2$
FNBUM3	" /forvar	0.38 (0.17 for formvar)	"	"	As FNBUM1
FNBUM4	"	"	"	"	As FNBUM2
NBTIC1	Evaporated Ti/Nb Ti/Nb ~ 0.28 (w/o)	0.54	"	"	Nominal thickness ~ 30 nm Area analyzed $\sim 1\ \mu m^2$
NBTIC2	"	"	2 mrad	18 mrad	"
FNBEP1	$Fe_{40}Ni_{40}B_{20}$ electropolished	0.20	"	5.8 mrad	
FNBEP2	"	0.98	"	"	B peak lost in background
SIODP1	SiO replica	0.4	"	"	
SIODP2	"	"	"	10 mrad	Same area as SIODP1
SIODP3	Ti(C,N)/SiO extraction replica	0.4	"	5.8 mrad	Cuboidal particle C:N $\sim 1:1$

TABLE I (cont'd)

Spectrum Number	Sample	Sample Thickness ($\frac{t}{\lambda}$)	Convergence Angle (α)	Collection Angle (β)	Notes
SIODP4	Ti(C,N)/SiO extraction replica	?	10 mrad	20 mrad	Cuboidal particle, ∿30-40 nm
CRB201	Chromium boride powder on holey C film	?	2 mrad	5.8 mrad	
CRB202	" "	"	"	"	thinner area
BNJT01	Boron nitride powder on holey C film	?	"	"	
BNJT02	"	?	"	"	same area as BNJT01
TIB201, 02,03,04	Titanium diboride on holey C film		"	"	Spectra from various thicknesses
MTGLS1	MetGlas (5.6 w/o B, 11.9 w/o P, 13 w/o Cr, 36 w/o Ni, balance Fe) - electropolished	0.45	"	"	Oxide film on surface?
MTGLS2	"	0.2	"	"	
B4C01, 02,03,04	Boron carbide on holey C film	0.8→0.3	"	"	
BATI01	Barium titanate, ion milled	0.22	"	"	8 year old sample

TABLE I (cont'd)

Spectrum Number	Sample	Sample Thickness ($\frac{t}{\lambda}$)	Convergence Angle (α)	Collection Angle (β)	Notes
BATIO2	Barium titanate, ion milled	0.25	2 mrad	5.8 mrad	L3 argon edge
NIOJT1	Nickel oxide, ion milled	0.16	"	"	
NIOJT2	"	0.74	"	"	zero loss saturated
NIOJT3	"	0.63	"	"	"
CR2NO1, 02,03	Chromium nitride, extraction replica	0.4	"	"	particles from alloy steel
M23C61,2	Carbide, extraction replica	0.5	"	"	"
PE1601, 02,03,04	Nimonic (43.5 Ni, 34.3 Fe, 16.5 Cr, 1.18 Ti, 1.15 Al, 3.17 Mo, 0.15 Si) - electropolished	0.14,0.35, 0.4,0.7	"	"	Solution treated
316JT1,2	316L Stainless (65.3 Fe, 17 Cr, 12.2 Ni) - electropolished	0.5,>0.5	"	"	Crept sample O,C peaks visible

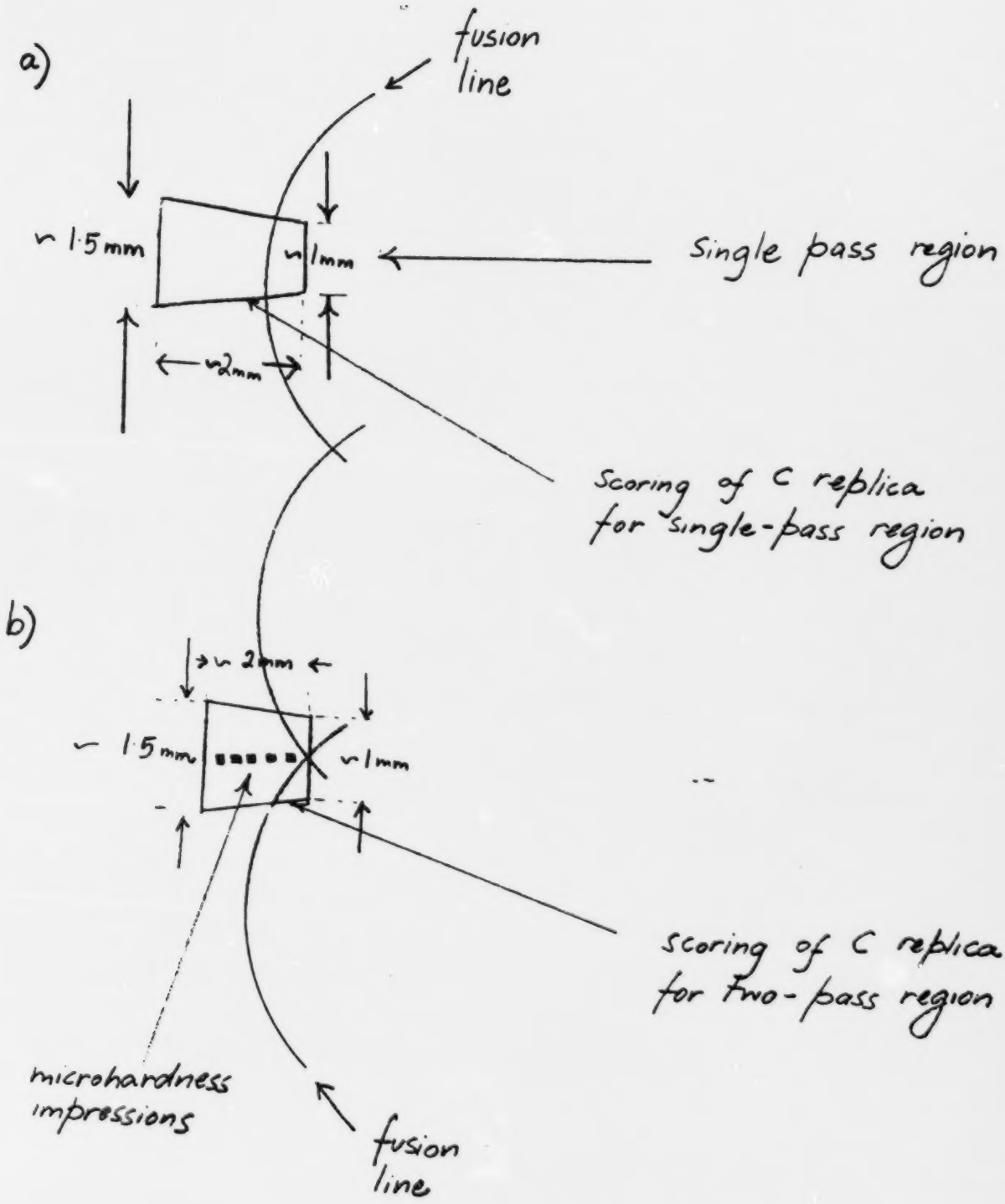

Fig. 16. Schematic diagram illustrating the method of carbon replica scoring in (a) single pass region of the weld, and (b) two pass region of the weld.